KfK 3286
März 1982

The CELLO Detector and LAr Calorimeters at PETRA

G. Flügge
Institut für Kern- und Teilchenphysik

Kernforschungszentrum Karlsruhe

KERNFORSCHUNGSZENTRUM KARLSRUHE

Institut für Kern- und Teilchenphysik

KfK 3286

The CELLO Detector and LAr Calorimeters at PETRA

G. Flügge

Kernforschungszentrum Karlsruhe GmbH, Karlsruhe

Kernforschungszentrum Karlsruhe GmbH
ISSN 0303-4003

The CELLO Detector and LAr Calorimeters at PETRA

ABSTRACT

The layout and performance of the CELLO detector at PETRA is described. In particular, its LAr calorimeter is presented in comparison with the TASSO shower detector. First experience with longterm stability and performance of LAr calorimeters at PETRA is discussed.

Der CELLO-Detektor und LAr-Kalorimeter bei PETRA

ZUSAMMENFASSUNG

Der Aufbau und die Arbeitsweise des CELLO-Detektors bei PETRA werden beschrieben. Insbesondere wird sein LAr-Kalorimeter dargestellt und mit dem TASSO-Schauerzähler verglichen. Erste Erfahrungen mit Langzeitstabilität und Betriebsdaten von LAr-Kalorimetern bei PETRA werden diskutiert.

1. INTRODUCTION

The CELLO detector[1] was designed to provide full solid angle coverage for

- final states including leptons ($e,\nu,\tau,...$)
- e^+e^- annihilation into hadrons (charged and neutral)
- two photon reactions with leptons and hadrons in the final state
- production and decay of heavy quarkonia, in particular cascade decays involving low energy photons.

To achieve this goal, nearly the full solid angle was instrumented for

- high precision charge particle tracking
- good electron and photon detection and e/h separation
- muon detection
- efficient triggering also on low mutliplicity and neutral energy.

Less emphasis was put on charged particle identification (π,K,p).

A layout of the detector[2] is shown in fig. 1. Its inner part consists of cylindrical proportional and drift chambers which measure charged particle tracks in the 1.3 T solenoidal field of a superconducting magnet. Outside the magnet a lead-liquid argon calorimeter provides photon and electron detection through electromagnetic showers.

The iron return yoke acts as a filter for muon/hadron separation. Muons penetrating the iron are detected in large area drift chambers outside the yoke. The different components are summarized in Table 1.

Fig. 2 shows two typical events taken at CELLO at highest PETRA energy. A cross section perpendicular to the beam is displayed. Charged tracks are visuallised by their hits in the cylindrical chamber and their computer reconstruction. The dashes in the liquid argon system correspond to electromagnetic energy deposits.

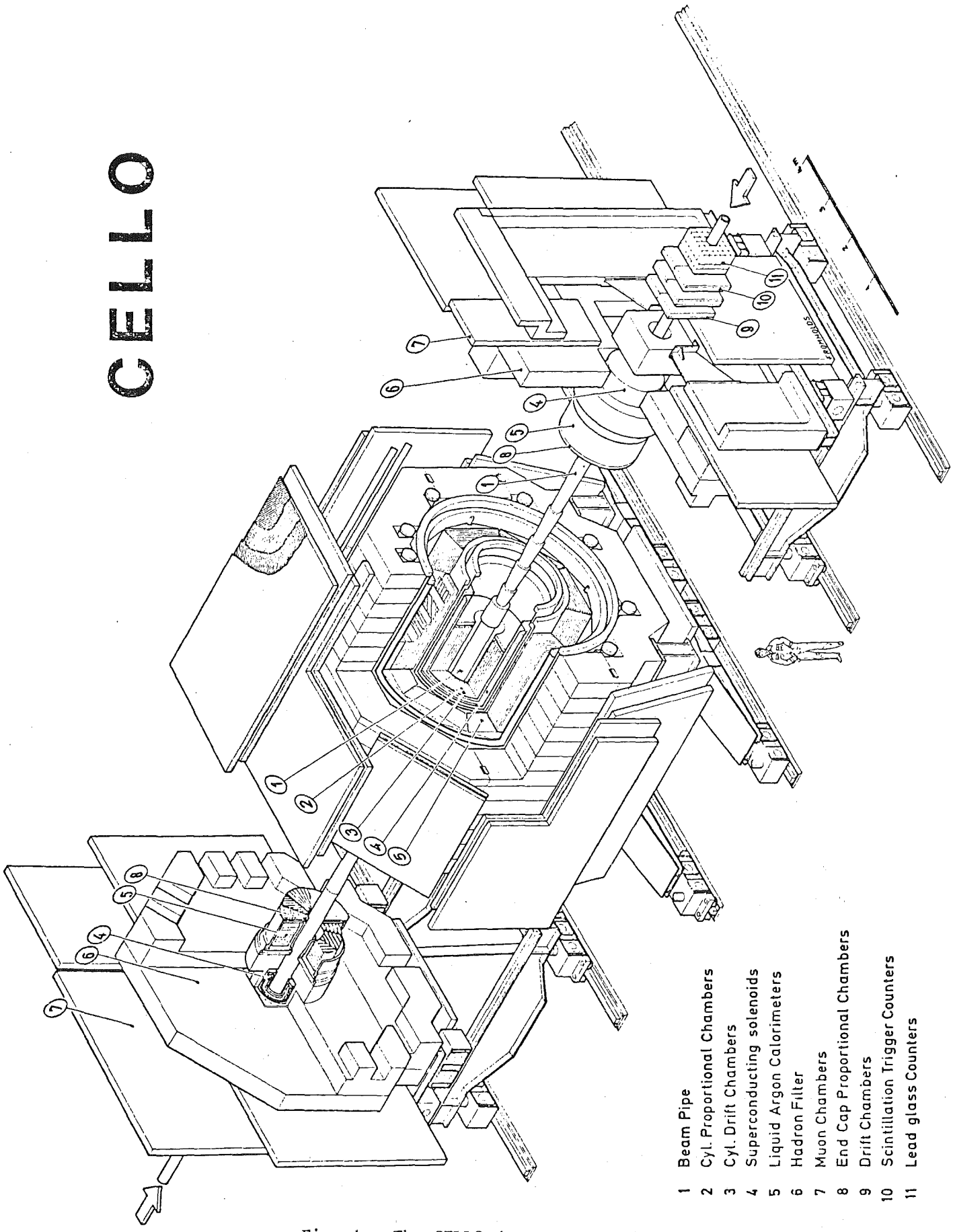

Fig. 1: The CELLO detector at PETRA

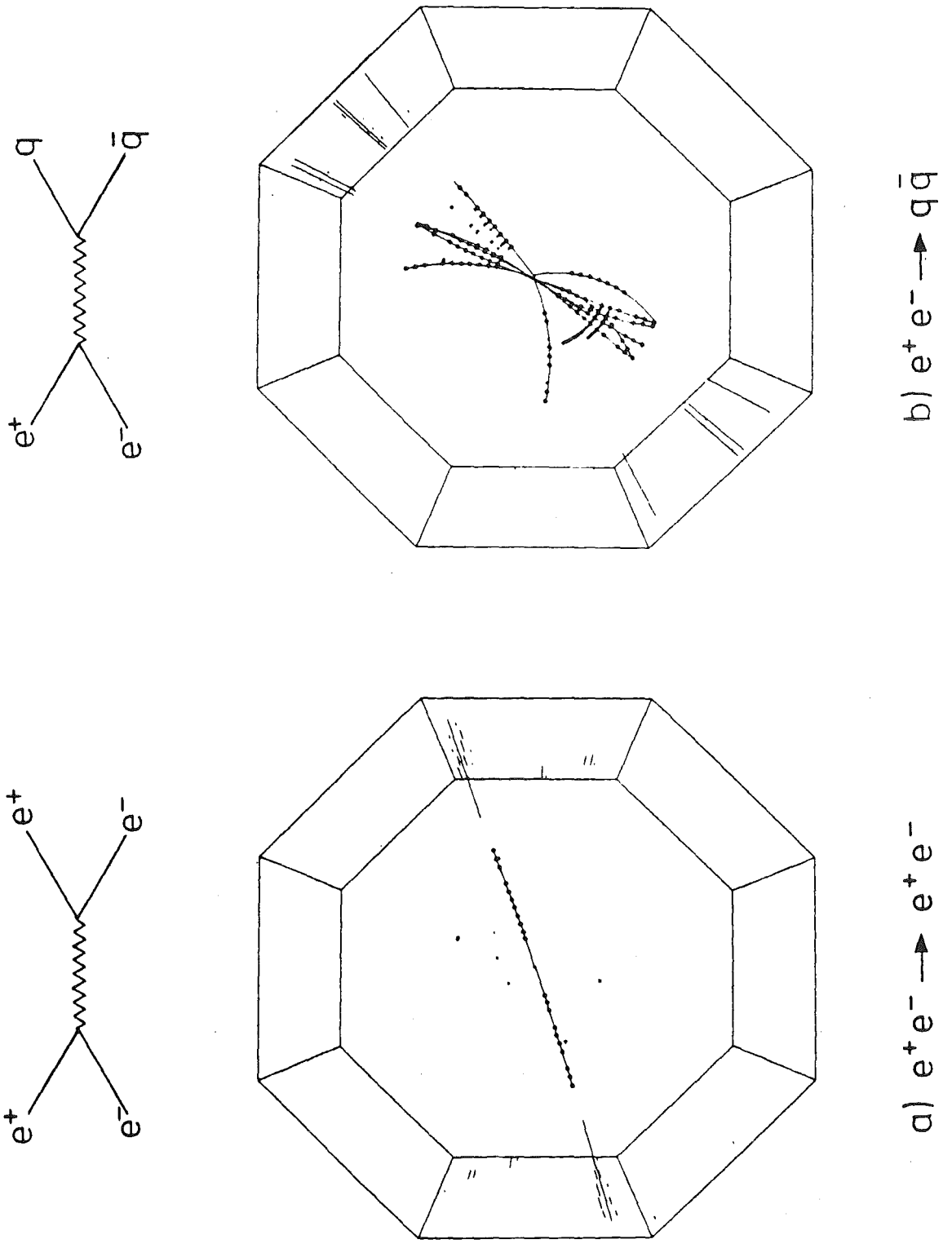

Fig. 2: Two typical events in the CELLO detector
a) elastic scattering
b) hadronic annihilation

Table 1: CELLO-components

Device	Modules	$\Delta\Omega/4\pi$	thickness X_o	dimensions (cm)	Performance
Tracking	5 cyl. PWC's 7 cyl. DC's	0.91	0.01	length 220 radius 17-70	σ_z = 440 μm $\sigma_{r\phi} \simeq$ 200 μm
	8 plan. PWC's	0.10		radius 21-66	
Solenoid			0.49	length 400 Ø 140	superconducting 1.3 T
LAr shower detector	16 cyl. 4 endcaps	0.96	20 21		$\sigma_{E/E} = 13\%/\sqrt{E}$ after 1 X_o
μ-chamber	32	0.92			σ = ±6 mm

Central Detector

The central tracking detector consists of cylindrical proportional and drift chambers mounted in a thin superconducting coil (0.49 X_o) which produces a solenoidal field of 1.3 T. The device combines

- good rϕ resolution of drift chambers and
- good z resolution, trackfinding and trigger abilities of proportional chambers with cathode readout.

The chamber arrangement is sketched in Fig. 3. One double and four single proportional chambers are interleaved with two double and one triple layer of drift chambers. They provide a visible track length of 53 cm. The drift chamber lever arm is rather short, only 39 cm. Adding a vertex chamber in front of PC1 would substantially improve the momentum resolution.

The inner detector covers 91% of the solid angle for particles with at least 8 points per track. It is complemented by 8 additional endcap proportional chambers subtending 10% of the solid angle.

Some parameters of the inner detector and its performance are summarized in Table 2. The problem of operating drift chambers of a simple cell structure in a high magnetic field has been solved satisfactorily. Details are given elsewhere and will be discussed in H. Boerner's talk[3]. The momentum resolution is $\sigma_{p_\perp/p_\perp}{}^2 = 2.9\%$ (2% including the interaction point).

The right-left ambiguity is resolved by the proportional chambers. Analog readout on the cathode strips (average effective width about 4.5 mm) running perpendicular and at 30^o to the sense wire provides an excellent z resolution of 440 μ (Fig. 4).

A combination of 5 proportional chambers and two drift chambers is used for triggering. Preselected patterns are compared to real events in a sophisticated programmable trackfinding logic based on random ac-

Table 2: CELLO Inner Detector

• Chambers:		5 PC + 7 DC
• Magnetic Field		1.3 T SC
• Sensitive Volume	length	220 cm
	radius	17 ÷ 70 cm
• Material in front		0.06 X_o
Material in detector		0.02 X_o

Drift Chambers:

• rφ resolution:	single wire	≈ 100 μm
	average over detect.	≈ 200 μm
	for large p	≈ 170 μm
• Momentum resol.	without IP	2.9%
$\sigma_{p_\perp/p_\perp^2}$	with IP	2.0%
• Angular resol.	σ_ϕ	3 mrad

Prop. Chambers:

• Z resolution	σ_z	440 μm
	σ_θ	2 mrad

Inner Detector:

Trigger:	2 rφ, 1 rz track →	< 1 Hz
Reconstr. efficiency:		~ 95%
Spurious tracks:	jets {	~ 1%
Reconstr. time:	1 track :	50 ms
	$\mu^+\mu^-$:	120 ms
	multihadron :	5 ÷ 10 s

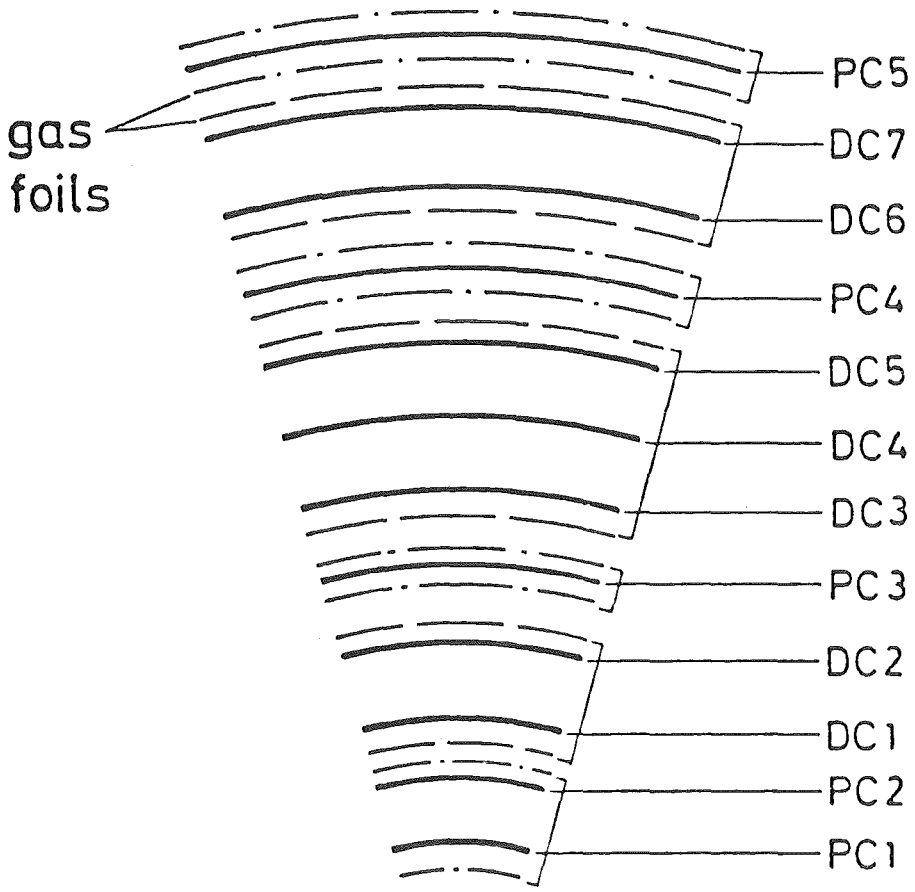

Fig. 3: Arrangement of drift and proportional chambers in the central detector.
PC1...5: proportional chambers
DC1...7: drift chambers

cess memory devices. Both rϕ and rz information is used. This allows for loose trigger requirement at acceptable rates (< 1 Hz): 2 tracks in rϕ and 1 track in rz.

Reconstruction efficiency and reconstruction time as given in Table 2 are comparable to other drift chamber detectors[3].

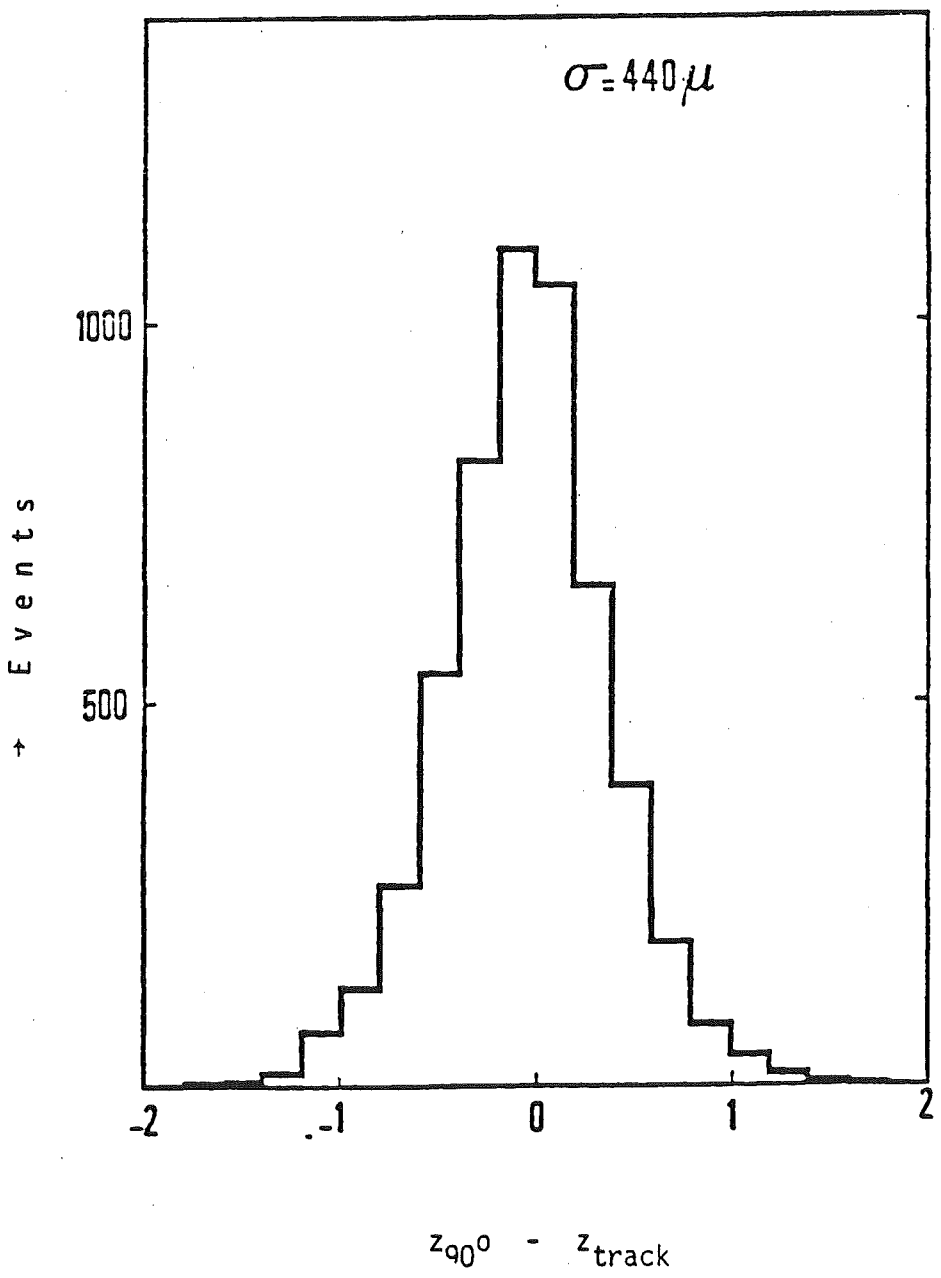

Fig. 4: Z-resolution from analog readout of cathode strips

LAr calorimeters at e^+e^- detectors

In table 3 some parameters of the three existing LAr calorimeters at e^+e^- machines are summarized[4,5]. As can be seen from this table, the largest solid angle coverage is achieved in the compact design of the CELLO detector. All barrel calorimeters are placed outside the magnet. CELLO profits from its very thin (0.49 X_o) superconducting coil.

Two groups (CELLO and MARK II) have chosen a strip structure for lateral shower sampling whereas TASSO has decided to combine strips and towers. There are obvious advantages in both cases:

- Easy pattern recognition in towers
- reduced number of channels in strip structures; or improved sampling for the same number of channels.

Consequently the longitudinal sampling is much finer in the first two detectors. Generally speaking, a proper combination of the two structures seems to be the optimal solution[6].

Fig. 5 shows the layout of the TASSO barrel counters. Small front towers and larger back towers are interleaved with strips for dE/dx measurement and improved shower location in two coordinates (z and ϕ).

The CELLO barrel shower counter will be described in some detail looking at Fig. 6. 16 modules of the type shown in the figure are mounted in one single cylindrical cryostat. This reduces the dead space between modules to 2%. Each module is coffin shaped, 2 m long and on average 1 m wide. The stack is made out of alternating Pb strips and plates (1-2 mm thick) interleaved with 3.6 mm gaps filled with liquid argon (LAr). There are 41 Pb/LAr double gaps and two additional 6 mm LAr gaps for dE/dx measurements. The total thickness of the module is 43 cm corresponding to 20 X_o. The 41 Pb layers are ganged into 6 readout channels in z direction (ϕ layers), 6 channels in φ direction (θ layers) and 5 channels at 45^o. These 17 longitudinal samplings are read out separately. The 6ϕ layers are also used for triggering (resolution of $18\%/\sqrt{E}$ on the trigger level).

Table 3: LAr Calorimeters in e^+e^- Detectors

	MARK II	CELLO	TASSO
Completion	1978	1980	1981
$\Delta\Omega/4\pi$	0.60	0.96	0.53
Weight		70 t	120 t
# Cryostats	8 barrel + 1 endcap	1 barrel + 2 endcaps	4 barrel + 2 endcaps
# Modules (barrel + endcap)	8 + 1	16 + 4	8 + 2
# Electr. Chann.	3200	7600 →(10700)*	14800
Barrel Calorimeters:			
Distance IP	165 cm	106 cm	180 cm
Material in front of active detector	1.3 X_o	0.7 X_o	1.5 X_o
Thickness	14 X_o	20 X_o	14 X_o
# dE/dx gaps	2 × 2	2 × 2	2 × 2
Longitudinal samplings	6	15(17)*	2
Lateral sampling	strips	strips	towers + strips

* For 1982 the number of electronic channels is being increased by 50%.

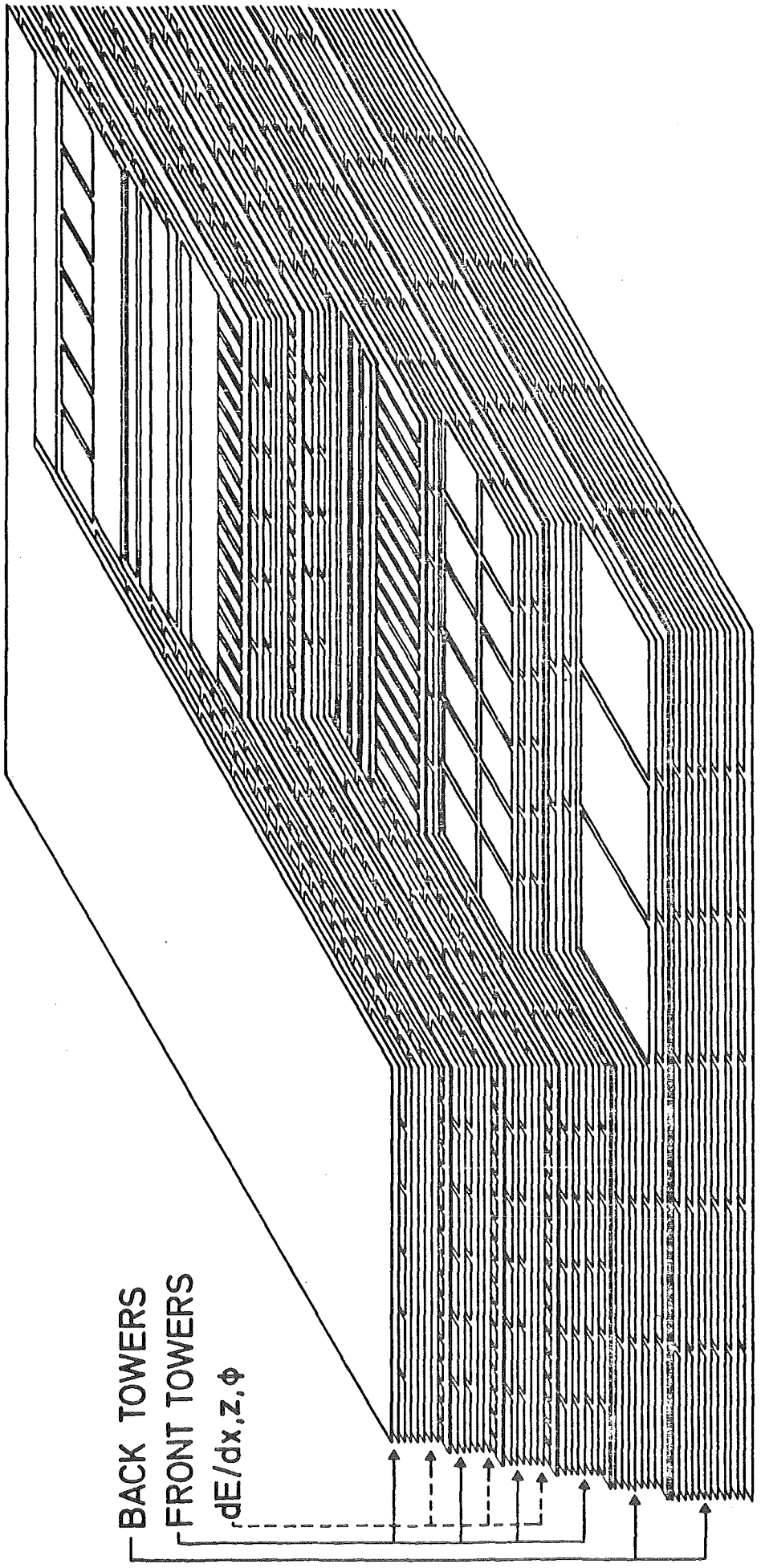

Fig. 5: TASSO barrel LAr calorimeter module

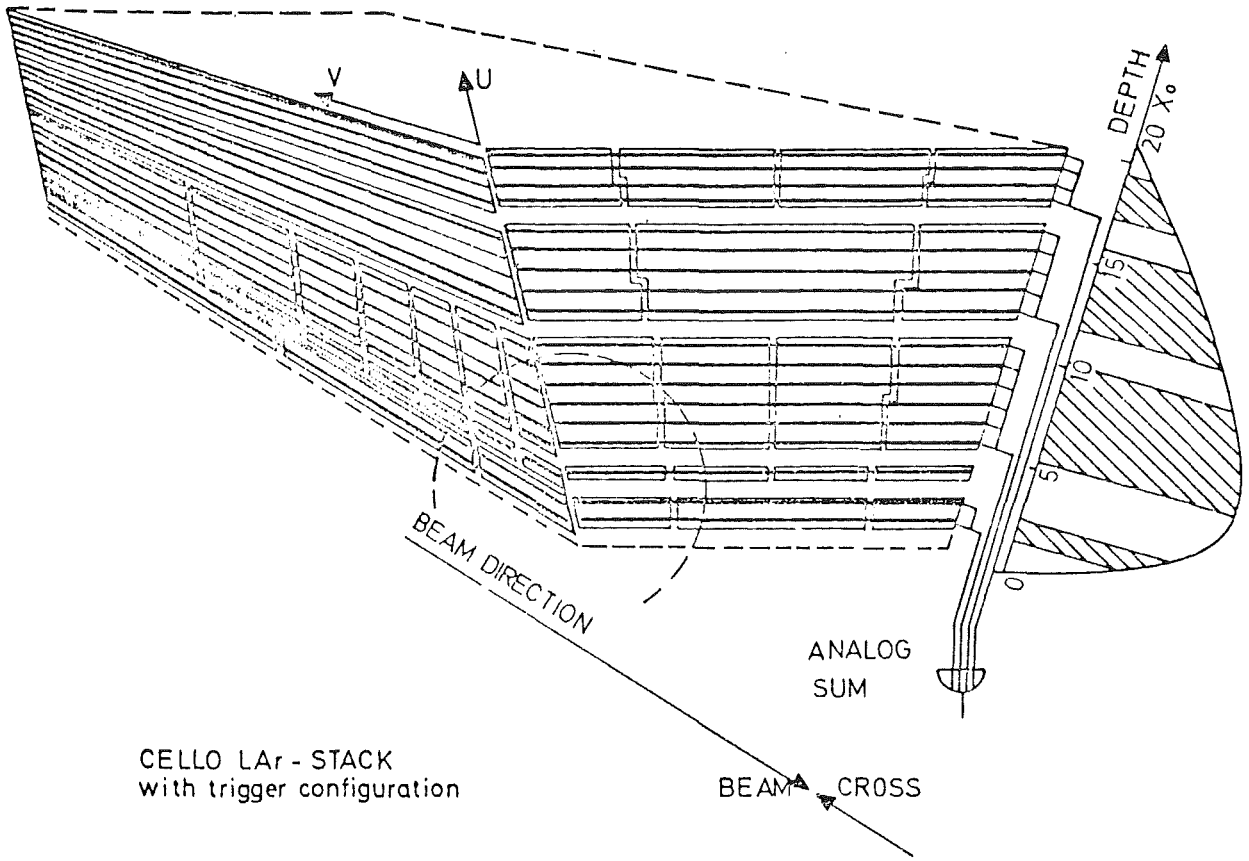

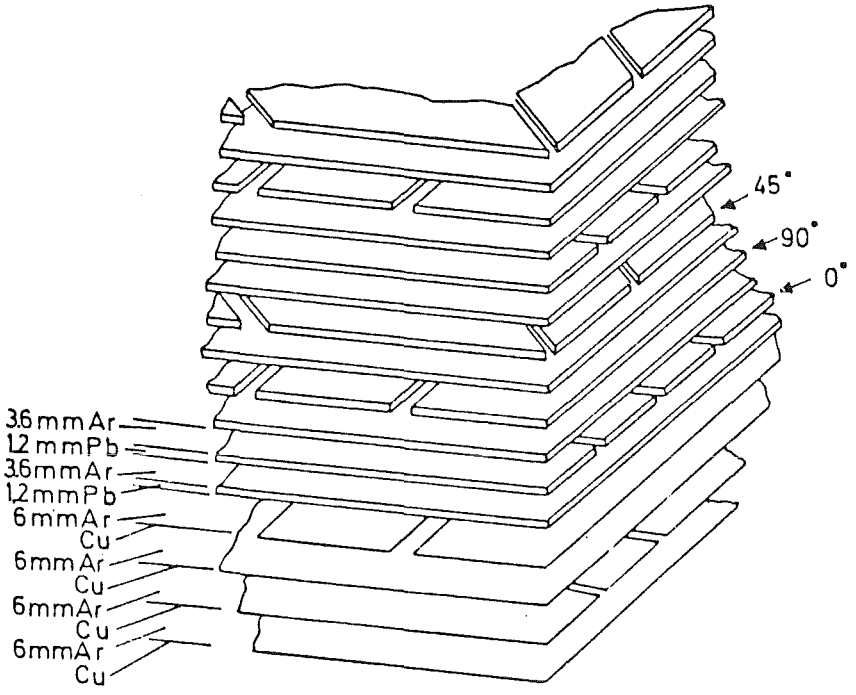

Fig. 6: CELLO barrel LAr calorimeter module

The cryogenics has - after some initial sealing problems - been stable for nearly 2 years of operation. The argon purity could be kept at a constant level of 1.3 ppm oxygen equivalent corresponding to about 80% charge collection.

The electronics contains 7600 channels (including endcaps) of low noise preamplifiers (noise 0.8 - 5 fC determined by channel capactitance and twisted pair cables), main amplifiers, ADC and readout logic (Fig.7). The total cost per channel was 100 DM (including cables, connectors, housing and power supplies). Presently the ganging of channel in the barrel calorimeter is changed and the total number of channels is increased to 10700.

Since the channel capacities are different, all channels are calibrated individually by induced signals at the preamplifier input (Fig. 7). The stability of pedestals and amplification are continuously checked. CELLO found that all variations stayed within the statistical fluctuations of the measurements over a time period of about two month; less than 1 ADC count on the pedestals, less than 2% on the amplification gain, and less than 1% on the total charge in bhabha events.

Some relevant performance parameters of the LAr calorimeters of the PETRA detectors CELLO and TASSO[7] are given in Table 4. For comparison the corresponding numbers for the lead glass counters of the JADE detector are also included[8].

The energy resolution in the CELLO calorimeter as determined from real data (Bhabhas and compton electrons) is shown in Fig. 8. The mean amount of material in front of the stacks was 1 X_o due to the LAr in the gaps between the stacks and the cryostat wall. The value of $\sigma_{E/E} = 13.3\%/\sqrt{E}$ determined from Fig. 8 agrees well with 13% determined in beam tests with 1 X_o material in front. Next year in the upgraded calorimeter the superfluous LAr will be displaced leaving only 0.7 X_o material in front of the stack. The expected resolution will then be $\sigma_{E/E} = 11 \div 12\%/\sqrt{E}$. A similar resolution is found for the TASSO LAr calori-

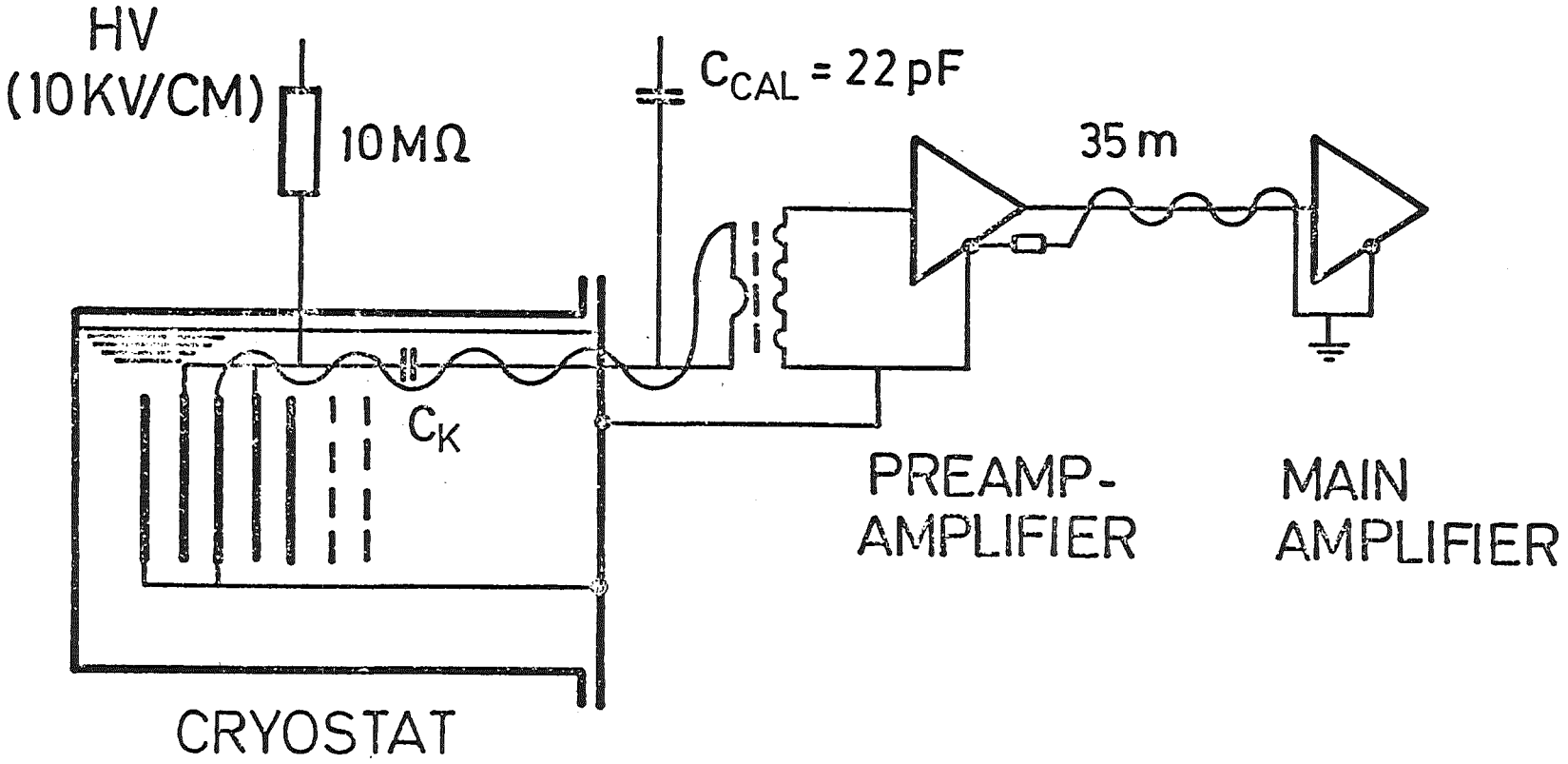

Fig. 7: Principle of the readout electronics for LAr calorimeters

Table 4: Performance of Electromagnetic calorimeters

	CELLO	TASSO	JADE
• Energy resol. $\sigma_{E/E}$ E in GeV	$\frac{13\%}{\sqrt{E}}$ $(\frac{11\div12}{\sqrt{E}})$*	$\frac{(11 + \frac{2}{E-0.5})\%}{\sqrt{E}}$	$\frac{4\%}{\sqrt{E}} + 1.5\%$
in energy range	0.4 ÷ 18.3 GeV	> 1 GeV	0.5 ÷ 2 GeV
σ_E for 17 GeV e^+e^-	3.2% ($\lesssim$ 3%)*	4.8%	2.4%
• Granularity (average)	20 mr ($\phi,\theta,45^o$)	35 mr towers 11 mr strips	75 mrad in ϕ 90 mrad in θ
$\sigma_\theta \simeq \sigma_\phi$ (E > 10 GeV)	4 mrad	3 mrad	7 mrad
2 photon separation	~ 50 mrad	~ 50 mrad	~ 150 mrad
• Mass res. $\sigma(M_{\pi^0})$	~ 23±5 MeV	22 ÷ 30 MeV	$\simeq$ 20 MeV
• Low energy γ eff.	100 MeV: $\simeq$ 90% test	160 MeV: $\gtrsim$ 90% MC	100 MeV: $\simeq$ 70% MC
• π/e separation	$4(2)^* \cdot 10^{-3}$ at 2 GeV/c and 90% e^- eff. (test)		$3.3 \cdot 10^{-2}$ at 2 GeV/c and 95% e^- eff. (test)
• signal noise (min.ion.))	$\gtrsim$ 5	30	> 50
• dE/dx (π,K-p)	< 1.2 GeV/c	< 1.2 GeV/c	
• Trigger	$\geq$ 2 × 0.5 GeV	$\Sigma \geq$ 4 GeV	$\Sigma \geq$ 4 GeV

* upgraded detector (1982)

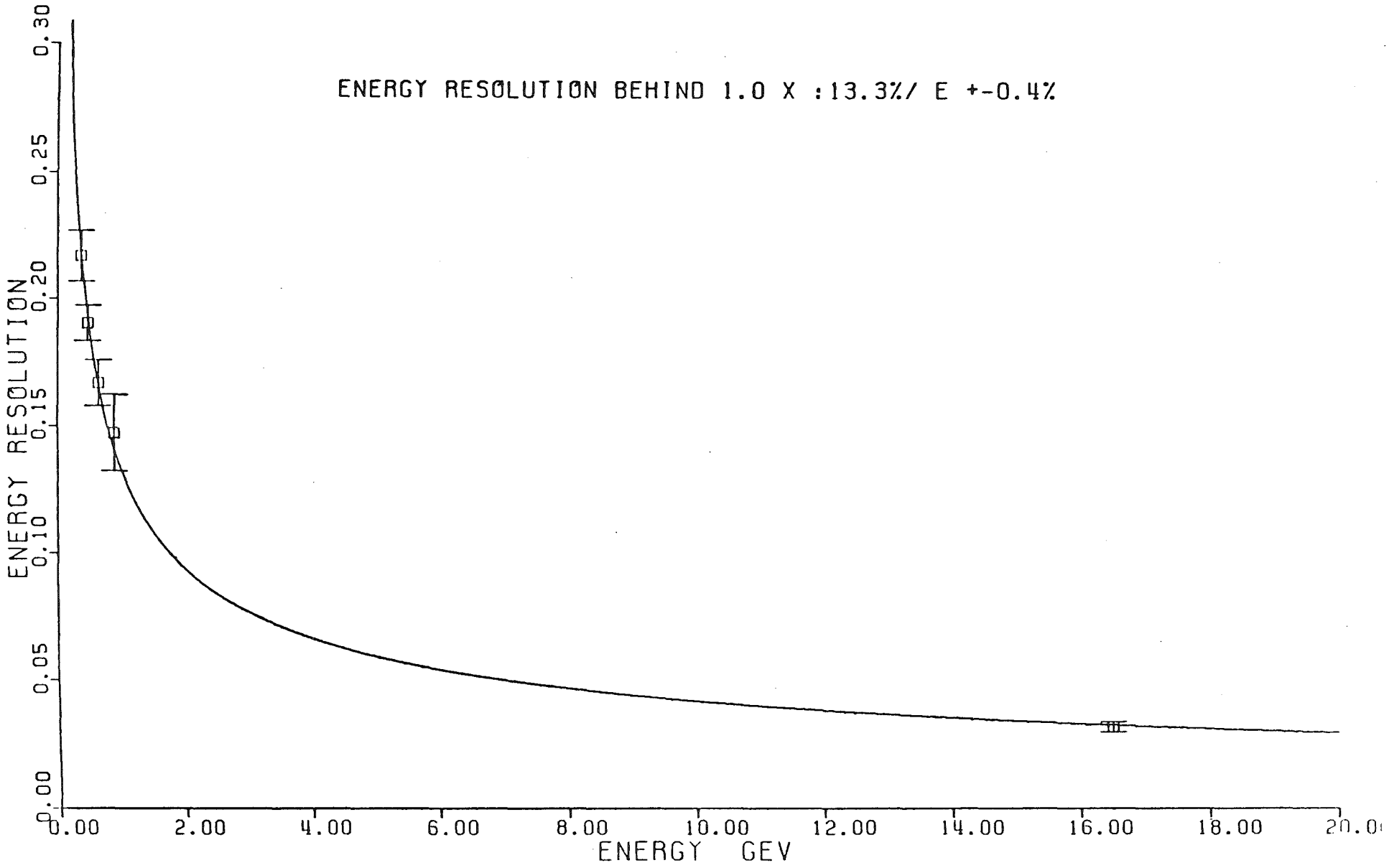

Fig. 8: Energy resolution of the CELLO LAr calorimeter

meter. The energy resolution in the lead glass system is better at low energy. At very high energies (> 18 GeV) both TASSO and JADE see a slight degradation due to leakage effects ($14 \pm 15\ X_o$ calorimeter thickness. The energy distribution for Bhabha events in the TASSO detector is shown in Fig. 9.

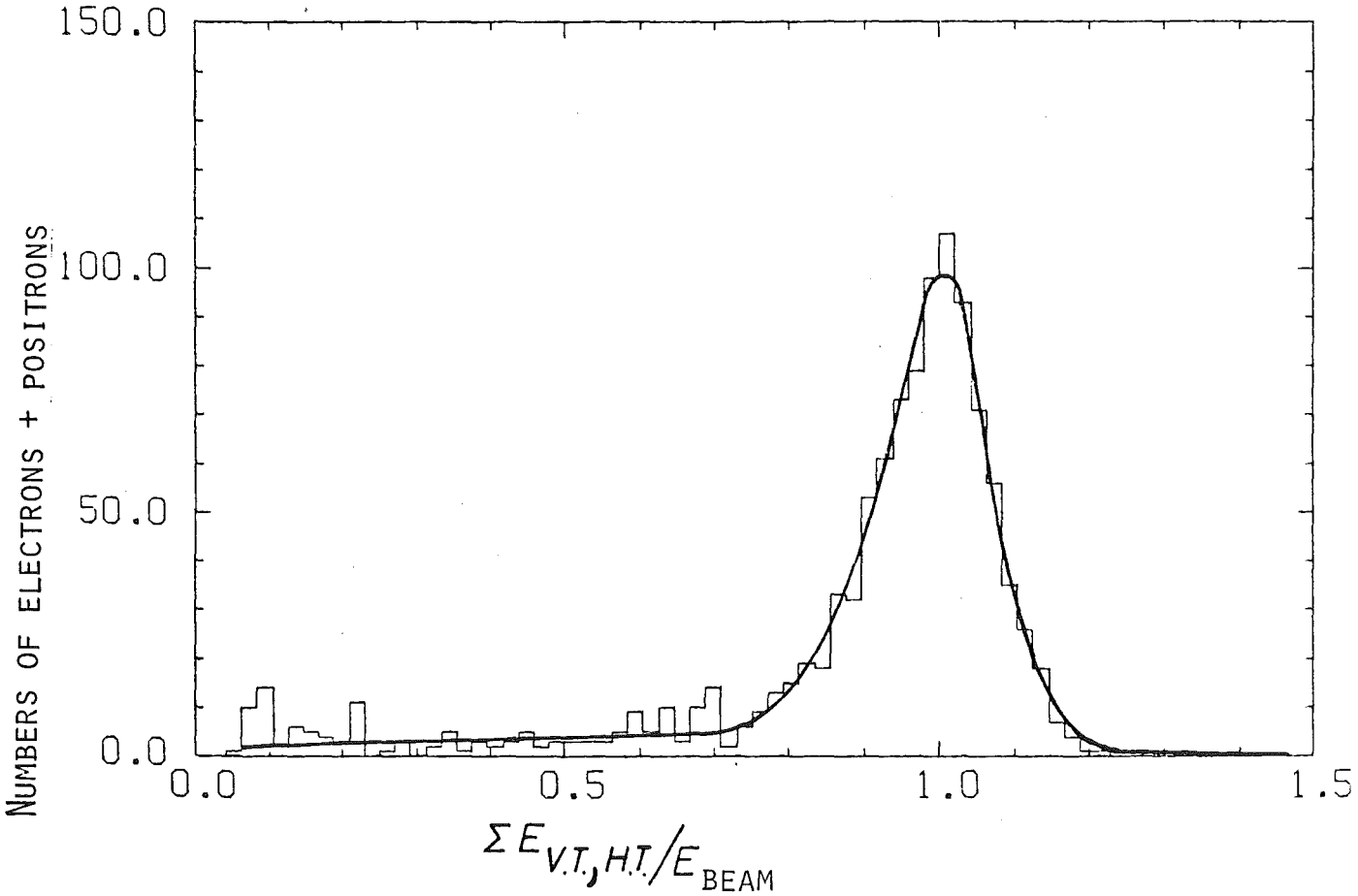

Fig. 9: Energy deposition of Bhabha events in the TASSO detector

The granularity is similar in the two LAr calorimeters and about two times worse in the JADE case. The angular resolution and two photon separation behave correspondingly. The π^0 mass resolution (Figs. 10 and 11) are again similar in both LAr detectors[7,9], reflecting again the similarity in energy and angular resolution.

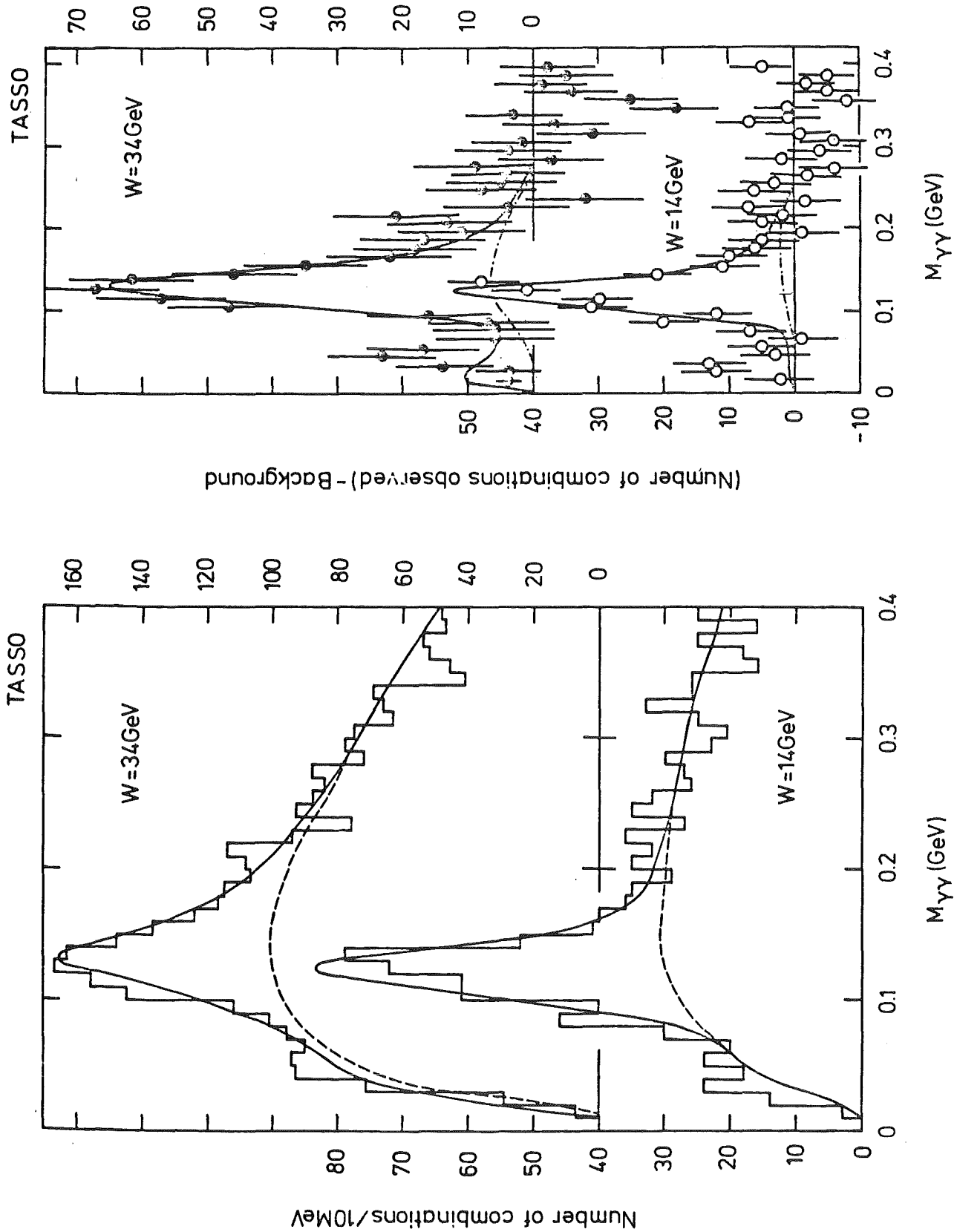

Fig. 10: $\gamma\gamma$ mass distribution for $E_\gamma > 0.15$ GeV at 14 and 34 GeV (TASSO)

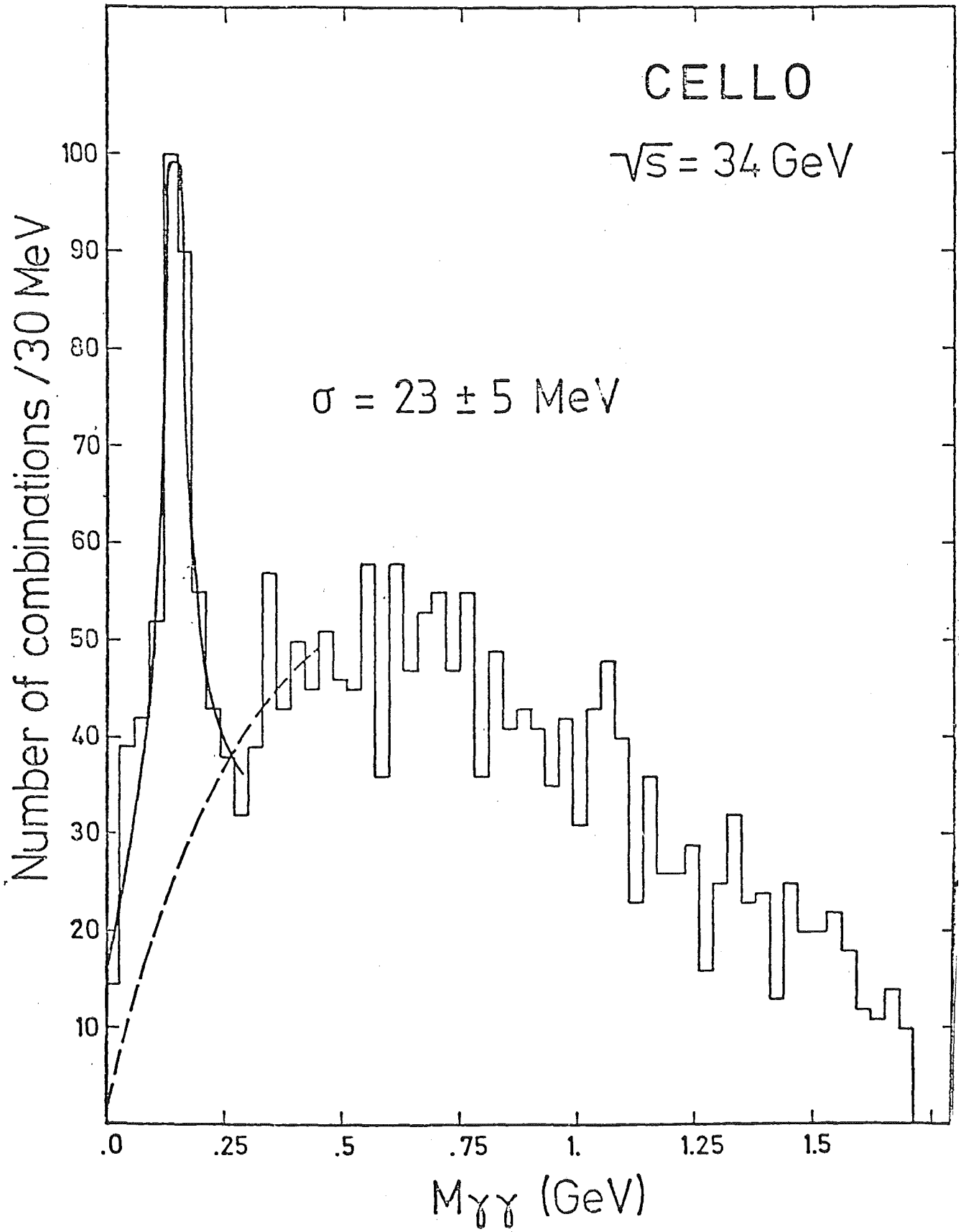

Fig. 11: $\gamma\gamma$ mass distribution for $E_\gamma > 0.3$ GeV at 34 GeV (CELLO)

Due to the thin coil, CELLO has good low energy photon efficiency. The numbers given for are test or Monte Carlo values.

The high longitudinal segmentation of the CELLO calorimeter enables a very good e/h separation. Tests showed a $4 \cdot 10^{-3}$ suppression of hadrons for momenta larger than 2 GeV/c and electron efficiencies of 90%. The rejection will improve to $2 \cdot 10^{-3}$ in the upgraded system.

In the signal to noise ratio the tower structure is clearly superior to the strip structure. Whereas CELLO has only minimum ionizing S/N ratios of 5 on channels with only one single strip, the corresponding numbers are 30 and > 50 in the TASSO and JADE case.

dE/dx separation for (π,k-p) is possible in both LAr detectors for momenta < 1.2 GeV/c.

Concluding Remarks

From experience with the CELLO detector and with LAr calorimeters at PETRA the following remarks may be appropriate:

Inner detector:

A simple drift cell structure of the MARK II type has proven to work reliably with good resolution even in a high magnetic field (1.3 T). An additional vertex detector yielding a high precision point close to the vertex would be desirable.

Proportional chambers with cathode readout proved extremely useful for triggeringin particular because they provide a z trigger. Their z resolution is not rivaled by any other detector except TPC. However, time consuming trackfinding remains an inherent problem for all detectores without space points.

LAr calorimeters:

No serious problems have been encountered in the cryogenics system. However, one has to keep in mind, that all time constants for setup and repair are long, of the order of 2-3 days (TASSO) or even weeks (CELLO) for cooldown and warmup. The experience in all LAr systems has been however, that after careful setup they are very stable and reliable both in the cryogenics and the electronics systems. No clear preference for strips or towers can be extracted from the existing performance parameters; an appropriate combination of both may be the optimal solution.

REFERENCES

1) CELLO Collaboration:
H.-J. Behrend, Ch. Chen, J. Field, U. Gümpel, V. Schröder, H. Sindt
Deutsches Elektronen-Synchrotron, Hamburg, Federal Republic of Germany

W.-D. Apel, J. Bodenkamp, D. Chrobaczek, J. Engler, D.C. Fries,
G. Flügge, G. Hopp, H. Müller, F. Mönnig, H. Randoll, G. Schmidt,
H. Schneider
Kernforschungszentrum and Universität Karlsruhe, Federal Republic of Germany

W. de Boer, G. Buschhorn, G. Grindhammer, P. Grosse-Wiesmann,
B. Gunderson, C. Kiesling, R. Kotthaus, U. Kruse, H. Lierl, D. Lüers,
T. Meyer, L. Moss, H. Oberlack, P. Schacht, M.-J. Schachter,
A. Snyder, H. Steiner
Max-Planck-Institut für Physik und Astrophysik, München, Federal Republic of Germany

G. Carnesecchi, A. Cordier, M. Davier, D. Fournier, J.F. Grivaz,
J. Haissinski, V. Journé, A. Klarsfeld, M. Cohen, F. Laplanche,
F. Le Diberder, U. Mallik, J.-J. Veillet, A. Weitsch
Laboratoire de l'Accélérateur Linéaire, Orsay, France

R. George, M. Goldberg, B. Grossetête, F. Kapusta, F. Kovacs,
G. London, L. Poggioli, M. Rivoal
Laboratoire de la Physique Nucléaire et Hautes Energies,
Paris, France

R. Aleksan, J. Bouchez, G. Cozzika, Y. Ducros, A. Gaidot, J. Pamela,
J.P. Pansart, F. Pierre
Centre d'Etudes Nucléaires, Saclay, France

2) CELLO Collaboration, H.-J. Behrend et al.,
Phys. Scipta 23 (1981) 610

3) W. de Boer et al., Nucl.Instr. and Meth. 156 (1978) 249 and
176 (1980) 167

H. Boerner, this workshop

4) H. Oberlack, General Meeting on LEP, Villars, 1981

5) P. Söding, General Meeting on LEP, Villars, 1981

6) A. Eisner et al., Report of the Subgroup on Calorimeter Geometries, SLAC, 1981, unpublished

7) TASSO Collaboration, R. Brandelik et al., DESY report 81-069 (October 1981)

8) S. Yamada, private communication

9) CELLO Collaboration, H.-J. Behrend et al., to be published